Acta Cryst E CRYSTALLOGRAPHIC COMMUNICATIONS

ISSN 2056-9890

Crystal and molecular structures of a binuclear mixed ligand complex of silver(I) with thiocyanate and 1*H*-1,2,4-triazole-5(4*H*)-thione

Janjira Kreaunakpan,[a] Kittipong Chainok,[b] Nathan R. Halcovitch,[c] Edward R. T. Tiekink,[d] Teerapong Pirojsirikul[a] and Saowanit Saithong[e]*

[a]Department of Chemistry, Faculty of Science, Prince of Songkla University, Hat Yai, Songkhla 90112, Thailand, [b]Materials and Textile Technology, Faculty of Science and Technology, Thammasat University, Khlong Luang, Pathum Thani, 12121, Thailand, [c]Department of Chemistry, Lancaster University, Lancaster LA1 4YB, United Kingdom, [d]Centre for Crystalline Materials, Faculty of Science and Technology, Sunway University, 47500 Bandar Sunway, Selangor Darul Ehsan, Malaysia, and [e]Department of Chemistry and Center of Excellence for Innovation in Chemistry, Faculty of Science, Prince of Songkla University, Hat Yai, Songkhla 90112, Thailand. *Correspondence e-mail: saowanit.sa@psu.ac.th

Received 26 November 2019
Accepted 4 December 2019

Edited by W. T. A. Harrison, University of Aberdeen, Scotland

Keywords: crystal structure; Ag^I complex; hydrogen bonding; 1*H*-1,2,4-triazole-5(4-*H*–thione); thiocyanate.

CCDC reference: 1969873

Supporting information: this article has supporting information at journals.iucr.org/e

The complete molecule of the binuclear title complex, bis[μ-1*H*-1,2,4-triazole-5(4*H*)-thione-κ^2S:*S*]bis{(thiocyanato-κS)[1*H*-1,2,4-triazole-5(4*H*)-thione-κS]-silver(I)}, $[Ag_2(SCN)_2(C_2H_3N_3S)_4]$, is generated by crystallographic inversion symmetry. The independent triazole-3-thione ligands employ the exocyclic-S atoms exclusively in coordination. One acts as a terminal S-ligand and the other in a bidentate (μ^2) bridging mode to provide a link between two Ag^I centres. Each Ag^I atom is also coordinated by a terminal S-bound thiocyanate ligand, resulting in a distorted AgS_4 tetrahedral coordination geometry. An intramolecular N—H···S(thiocyanate) hydrogen bond is noted. In the crystal, amine-N—H···S(thione), N—H···N(triazolyl) and N—H···N(thiocyanate) hydrogen bonds give rise to a three-dimensional architecture. The packing is consolidated by triazolyl-C—H···S(thiocyanate), triazolyl-C—H···N(thiocyanate) and S···S [3.2463 (9) Å] interactions as well as face-to-face π–π stacking between the independent triazolyl rings [inter-centroid separation = 3.4444 (15) Å]. An analysis of the calculated Hirshfeld surfaces shows the three major contributors are due to N···H/H···N, S···H/H···S and C···H/H···C contacts, at 35.8, 19.4 and 12.7%, respectively; H···H contacts contribute only 7.6% to the overall surface.

1. Chemical context

The title binuclear Ag^I complex, (I), containing 1*H*-1,2,4-triazole-5(4*H*-thione) and thiocyanate ligands has been synthesized and its crystal and molecular structures determined as part of our on-going studies in this area (Kodcharat *et al.*, 2013). Interest in the 1,2,4-triazole-based heterocyclic thione derives from the various medical applications and extensive biological activity exhibited by Schiff base molecules derived from 1,2,4-triazoles. For example, these molecules are known for their anti-fungal, anti-bacterial, anti-tumour, anti-convulsant, anti-inflammatory and analgesic properties (Al-Soud *et al.*, 2003; Walczak *et al.*, 2004; Almasirad *et al.*, 2004; Amir & Shikha, 2004; Turan-Zitouni *et al.*, 2005). In addition, the synthesis and biological activities of coordination complexes of these molecules continue to attract significant attention as coordination often enhances the biological activity of the organic molecules (Dharmaraj *et al.*, 2001; Singh *et al.*, 2006; Altundas *et al.*, 2010; Amer *et al.*, 2013; Bheeter *et al.*, 2016).

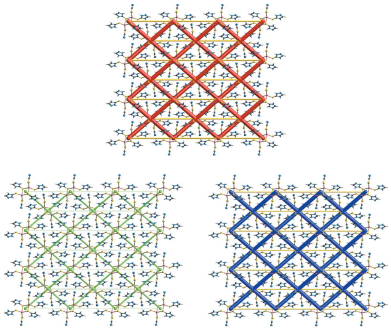

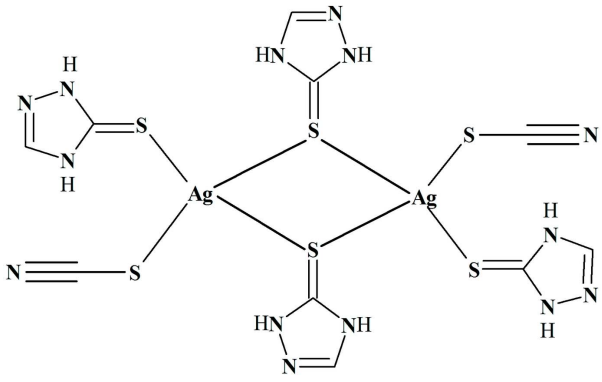

1*H*-1,2,4-Triazole-5(4*H*-thione), the heterocyclic ligand in (I) and hereafter referred to as HtrzSH, has attracted relatively little attention in the literature although recently the anti-cancer potential of derivatives of this were described (Büyükekşi *et al.*, 2018). The crystallographic study of (I) described herein is complemented by an analysis of the calculated HOMO and LUMO and an analysis of the calculated Hirshfeld surfaces and energy frameworks.

2. Structural commentary

The binuclear complex, $[Ag(HtrzSH)_2(SCN)]_2$ (I), Fig. 1, crystallizes in the monoclinic space group $P2_1/n$ and is disposed about a crystallographic centre of inversion. The HtrzSH molecules only employ their exocyclic thione-sulfur atoms in coordination, there being no Ag···N contacts of note. Each Ag^I atom is coordinated by a terminally bound HtrzSH molecule and by two thione-sulfur atoms derived from two μ_2-bridging HtrzSH molecules. The coordination of each Ag^I atom is completed by a terminal, S-bound thiocyanate anion. The geometry around the silver centre defined by the S_4 donor set is distorted tetrahedral with the S—Ag—S bond angles spanning about 25°, *i.e.* from a narrow 91.60 (2)° for S1—Ag—S1^i, being subtended by the bridging S1 atoms, to a wide 127.43 (2)° for S2—Ag—S3; symmetry operation (i): $1-x, 1-y, 1-z$. The Ag_2S_2 core has the shape of a distorted rhombus as the Ag—S1 bond length of 2.5596 (7) Å is significantly shorter than the Ag—S1^i bond of 2.8188 (7) Å. The Ag—S bond lengths fall in two distinct classes, with the Ag—$S1_b$ and Ag—S_t (b = bridging, t = thiocyanate) bond lengths being similar and shorter than Ag—$S1^i_b$ (Table 1). Despite the different modes of coordination of the thione-S atoms, the C1—S1 and C3—S2 bond lengths are indistinguishable at 1.698 (3) Å. Each of the C1—S1 and C3—S2 bond lengths in (I) are marginally longer than 1.6836 (19) Å found in the structure of the free molecule (Büyükekşi *et al.*, 2018). This small difference is reflected in the observation that no significant differences are evident in bond lengths within the five-membered rings in (I) and those in the uncomplexed molecule (Büyükekşi *et al.*, 2018).

The five-membered rings lie prime to either side of the Ag_2S_2 core, with the dihedral angles between the core and the N1- and N4-rings being 88.99 (11) and 85.16 (11)°, respectively. The independent rings are close to being co-planar, exhibiting a dihedral angle of 8.38 (16)°. Finally, the N1-amine is orientated to be in close proximity to the S3-thiocyanato atom, enabling the formation of an intramolecular amine-N—H···S(thiocyanato) hydrogen bond (Table 2). While the N4-amine is similarly oriented, the H···S separation of 3.31 Å is not indicative of a significant interaction.

Table 1
Selected geometric parameters (Å, °).

Ag—S1	2.5596 (7)	C1—S1	1.698 (3)
Ag—S2	2.5103 (6)	C3—S2	1.698 (3)
Ag—S3	2.5374 (7)	C5—S3	1.660 (3)
Ag—S1^i	2.8188 (7)		
S1—Ag—S2	112.49 (2)	S2—Ag—S3	127.43 (2)
S1—Ag—S3	114.64 (2)	S2—Ag—S1^i	99.56 (2)
S1—Ag—S1^i	91.60 (2)	S3—Ag—S1^i	101.08 (2)

Symmetry code: (i) $-x+1, -y+1, -z+1$.

Table 2
Hydrogen-bond geometry (Å, °).

D—H···*A*	*D*—H	H···*A*	*D*···*A*	*D*—H···*A*
N1—H1*N*···S3	0.88 (1)	2.72 (2)	3.555 (2)	161 (3)
N1—H1*N*···N5^{ii}	0.88 (3)	2.57 (4)	3.023 (3)	113
N3—H3*N*···S2^{iii}	0.88 (1)	2.56 (2)	3.345 (2)	150 (3)
N4—H4*N*···N2^{iv}	0.80 (4)	2.38 (4)	2.900 (3)	123 (3)
N6—H6*N*···N7^{v}	0.88 (1)	2.03 (1)	2.877 (3)	163 (3)
C2—H2···S3^{ii}	0.89 (4)	2.87 (4)	3.504 (3)	129 (3)
C2—H2···N7^{vi}	0.89 (4)	2.66 (3)	3.184 (4)	118 (3)
C4—H4···N7^{vii}	0.91 (4)	2.58 (4)	3.306 (4)	137 (3)

Symmetry codes: (ii) $-x+\frac{1}{2}, y+\frac{1}{2}, -z+\frac{3}{2}$; (iii) $-x+2, -y+1, -z+1$; (iv) $-x+\frac{1}{2}, y-\frac{1}{2}, -z+\frac{3}{2}$; (v) $x+\frac{1}{2}, -y+\frac{1}{2}, z-\frac{1}{2}$; (vi) $-x+\frac{3}{2}, y+\frac{1}{2}, -z+\frac{3}{2}$; (vii) $-x+\frac{3}{2}, y-\frac{1}{2}, -z+\frac{3}{2}$.

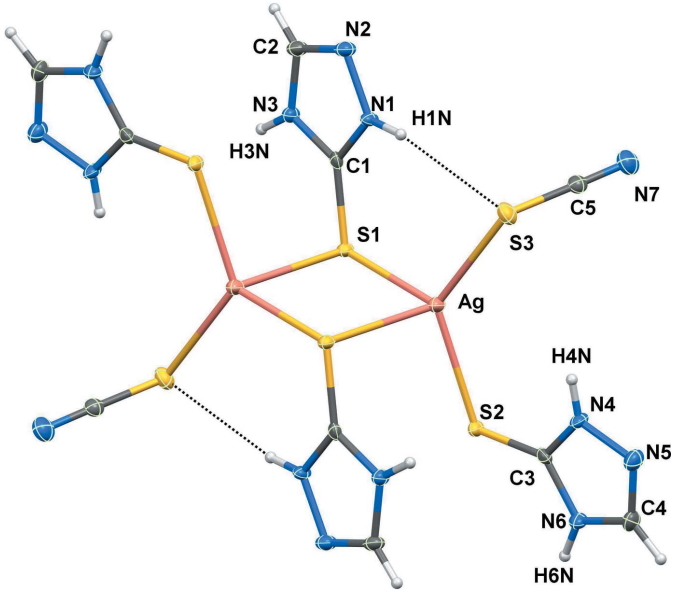

Figure 1
The molecular structure of (I) showing displacement ellipsoids at the 70% probability level. The unlabelled atoms are generated by the symmetry operation $1-x, 1-y, 1-z$. The dashed lines represent intramolecular amine-N—H···S(thiocyanato) hydrogen bonds.

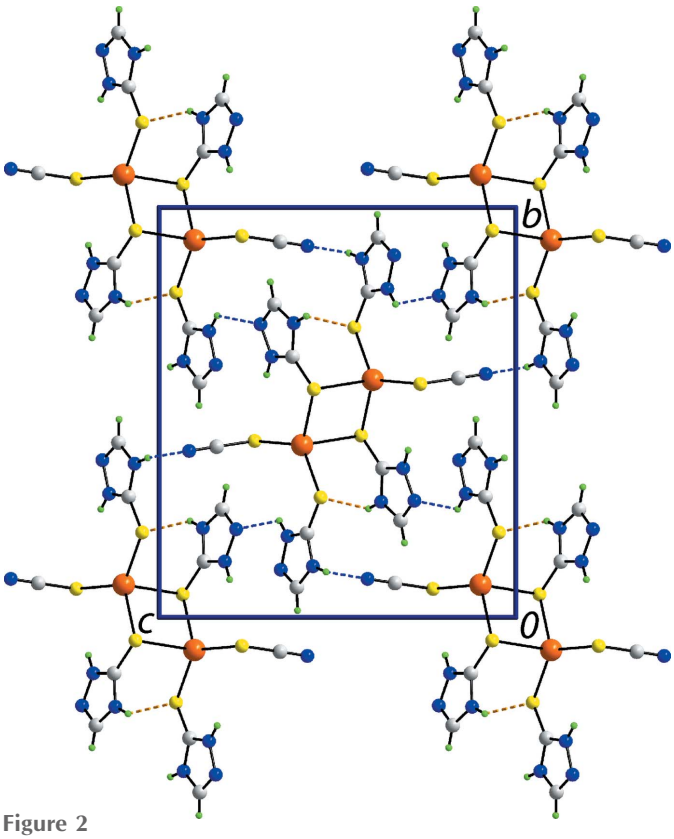

Figure 2
A view of the unit-cell contents of (I) in projection down the *a* axis, with N—H···S and N—H···N hydrogen bonds shown as orange and blue dashed lines, respectively.

3. Supramolecular features

The crystal of (I) consists of a three-dimensional network of hydrogen bonds and other non-covalent contacts as summarized in Table 2. The second amine-N—H atom of the S1-thione molecule [the first is engaged in an intramolecular N—H···S(thiocyanate) hydrogen bond and a second, weaker N—H···N5(triazolyl) interaction] forms a hydrogen bond to the thione-S2 atom. By contrast, the amine-N—H atoms of the S2-thione molecule form N—H···N(triazolyl) and N—H···N(thiocyanate) hydrogen bonds. The hydrogen bonds combine to sustain a three-dimensional architecture as shown in Fig. 2. Further stability to the molecular packing is provided by triazolyl-C—H···S(thiocyanate) and triazolyl-C—H···N(thiocyanate) interactions along with face-to-face π–π stacking (Fig. 3). The latter occur between the independent triazolyl rings [inter-centroid separation: (N1–N3,C1,C2)···(N4–N6,C3,C4)^{ii} = 3.4444 (15) Å and angle of inclination = 6.81 (16)° for (ii) $\frac{3}{2} - x, \frac{1}{2} + y, \frac{3}{2} - z$].

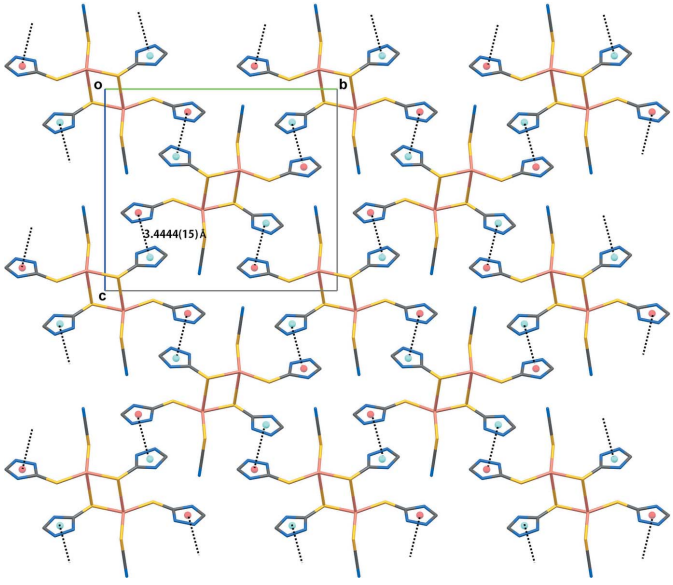

Figure 3
The face-to-face π–π stacking of (I).

4. Analysis of the Hirshfeld surfaces

The Hirshfeld surface analysis (McKinnon *et al.*, 2004; Tan *et al.*, 2019) of (I) was performed using *Crystal Explorer 17* (Turner *et al.*, 2017) to give further insight into the important intermolecular contacts normalized by van der Waals radii through a red–white–blue surface colour scheme where these colours denote the close contacts shorter than, equal to and longer than the sum of the respective van der Waals radii.

As seen in Fig. 4(*a*) of the Hirshfeld surface plotted over d_{norm} for (I), the red regions of the surface represent close contacts corresponding to the N—H···S and N—H···N hydrogen-bonding interactions mentioned above. An additional feature, *i.e.* S···S contacts, are noted. The closest of these, *i.e.* S1···S1^{iii} = 3.2463 (9) Å [symmetry operation: (iii) $2 - x, 1 - y, 1 - z$], link the binuclear molecules into chains along the *a*-axis direction. On the Hirshfeld surface mapped over electrostatic potential (DFT 3-21G) shown in Fig. 4(*b*), the faint-red and light-blue regions correspond to negative and positive electrostatic potential, respectively,

The full and delineated (H···H, N···H/H···N, S···S, S···H/H···S and C···H/H···C) two-dimensional fingerprint plots are shown in Fig. 5(*a*)–(*f*), respectively. The N···H/H···N contacts, at 35.8%, are the major contributor to the Hirshfeld surface. The S···H/H···S contacts (19.4%) also make a significant contribution. Other significant contributions come from the C···H/H···C (12.7%) and S···S (8.3%) contacts with H···H contacts, occurring at distances beyond the sum of the van der Waals radii, contributing only 7.6%. The next most significant contribution is made by N···C/

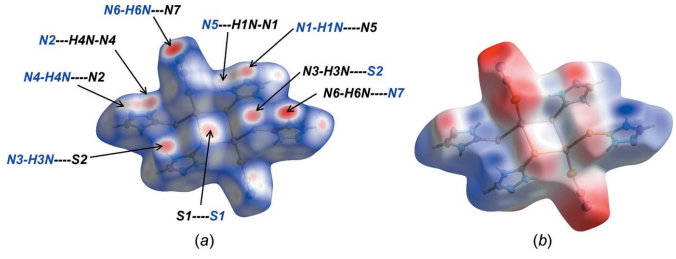

Figure 4
A view of the Hirshfeld surface for (I) mapped over (*a*) d_{norm} and (*b*) the electrostatic potential; the red and blue regions represent negative and positive electrostatic potentials, respectively.

Table 3
Summary of interaction energies (kJ mol^{-1}) calculated for (I).

R (Å)	E_{ele}	E_{pol}	E_{dis}	E_{rep}	E_{tot}	Symmetry operation
11.06	−142.4	−31.6	−39.9	77.9	−138.4	$\frac{1}{2}-x,\frac{1}{2}+y,\frac{1}{2}-z$
10.68	−89.0	−31.2	−54.8	43.5	−125.0	$\frac{1}{2}-x,\frac{1}{2}+y,\frac{1}{2}-z$
4.87	−50.3	−50.1	−120.3	176.8	−48.9	x, y, z
16.68	22.9	−3.0	−1.8	0.0	19.8	x, y, z
15.95	42.9	−7.4	−7.5	0.8	32.8	x, y, z

C···N contacts (6.7%) arising in the main from the π–π stacking interactions between triazolyl rings.

The energy frameworks were simulated (Turner *et al.*, 2017) in order to analyse the specific intermolecular interactions identified above for each molecule-to-molecule contact. This was achieved by summing up four different energy components (Turner *et al.*, 2017) for each pair of molecules, *i.e.* electrostatic (E_{ele}), polarization (E_{pol}), dispersion (E_{dis}) and exchange–repulsion (E_{rep}); these were obtained using the wave function calculated at the HF/3-21G level of theory. The results are summarized in Table 3. The greatest energy of attraction between molecules amounts to 138.4 kJ mol^{-1}, having a major electrostatic contribution (−142.4 kJ mol^{-1}), and is associated with the following interatomic contacts: C2—H2···N7, C4—H4···N7 and π–π stacking of between triazole rings. The next most significant contribution, with a total energy of −125.0 kJ mol^{-1}, arises from conventional hydrogen bonds, *i.e.* N1—H1*N*···N5, N4—H4*N*···N2 and N6—H6*N*···N7 as well as C2—H2···S3 interactions. The next attractive interaction, with E_{tot} = −48.9 and E_{dis} = −120.3 kJ mol^{-1}, respectively, reflects the N3—H3*N*···S2 hydrogen bonding and S1···S1 secondary bonding contact.

The magnitudes of intermolecular energies, *i.e.* the E_{ele}, E_{dis} and E_{tot} components, are represented graphically in Fig. 6(*a*)–(*c*), respectively, by energy framework diagrams whereby the cylinders join the centroids of molecular pairs using a red, green and blue colour scheme; the radius of the cylinder is proportional to the magnitude of interaction energy.

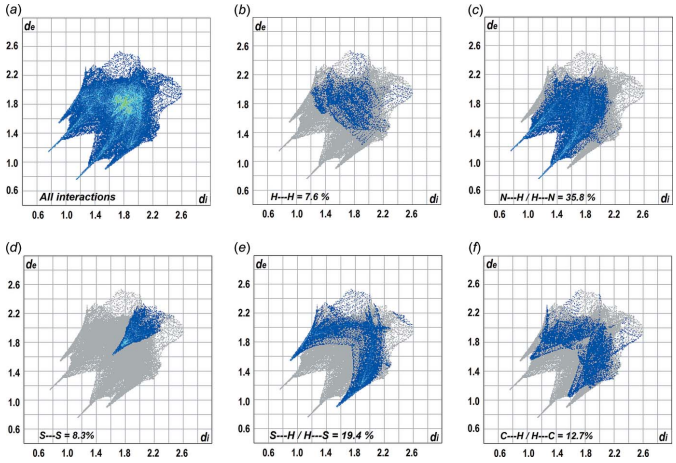

Figure 5
(*a*) A comparison of the full two-dimensional fingerprint plot for (I) and those delineated into (*b*) H···H, (*c*) N···H/H···N, (*d*) S···S, (*e*) S···H/H···S and (*f*) C···H/H···C contacts.

5. Molecular orbital calculations

The HOMO and LUMO energies for the atom positions in the crystal structure of (I) were calculated using a pseudopotential plane-wave DFT method (Parr & Yang, 1994) implemented in the *NWChem* package (Valiev *et al.*, 2010). The plane wave basis set and PBE exchange-correlation functional were chosen for the calculations on the experimental structure, *i.e.* without geometry optimization. The HOMO and LUMO of (I) are illustrated in Fig. S1 in the supporting information and their energies were calculated to be 3.011 and 6.173 eV, respectively. The HOMO is delocalized across the thiocyanato groups and the bridging region between the two dimers. The LUMO includes the delocalization around the triazole rings.

6. Database survey

A survey of the Cambridge Structural Database (Groom *et al.*, 2016) for coordination complexes of HtrzSH yielded seven structures. Monodentate coordination *via* the thione-S atom, as in (I), has been identified in six structures. The first three of these are neutral and mononuclear, namely $[(Ph_3P)_2Cu(HtrzSH)Cl]\cdot CH_3CN$, (NEPPOP; Wani *et al.*, 2013), $[Ag(HtrzSH)(NO_3)]\cdot CH_3OH$ (GISHUN; Wattanakanjana *et al.*, 2014) and $[Cd(HtrzSH)(H_2Edta)]\cdot H_2O$ (LOFKAT; Zhang *et al.*, 2008); H_4Edta is ethylenediamine tetracarboxylic acid. The mononuclear Fe^{III} complex, $Fe(NO)_2(HtrzS)(HtrzSH)\cdot 0.5H_2O$ (EYABOV01; Aldoshin *et al.*, 2008) contains both neutral and mono-anionic forms of HtrzSH. The fifth structure featuring monodentate coordina-

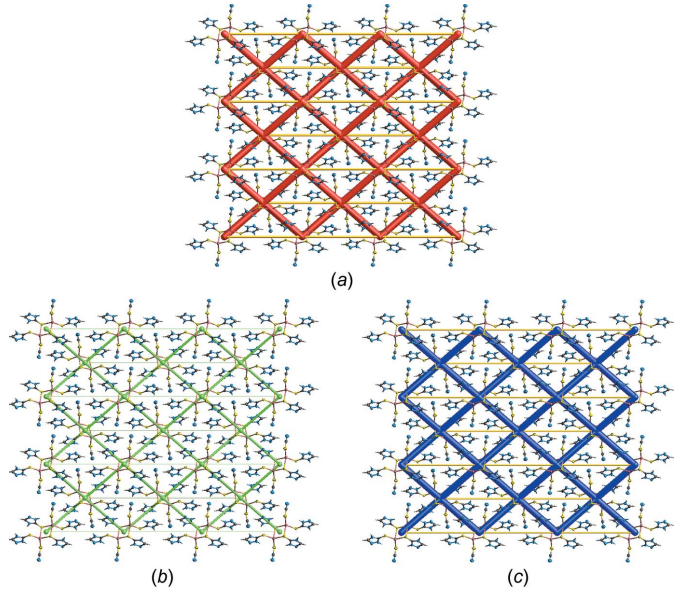

Figure 6
The colour interaction mapping and energy frameworks for (I) showing the (*a*) electrostatic potential force, (*b*) dispersion force and (*c*) total energy diagrams. All cylindrical radii were adjusted to the same scale factor of 100 with a cut-off value of −50.0 kJ mol^{-1} within a 3 × 3 × 3 unit cell and their sizes are proportional to the relative strength of the corresponding energies.

tion of HtrzSH is a two-dimensional coordination polymer, *i.e.* $\{[Cd_2(O_2CCO_2)_2(HtrzSH)_2]\cdot 2H_2O\}_n$ (ZIVBOX; Liang *et al.*, 2014); there are two distinct Cd^{II} atom coordination environments. Two distinct coordination modes for HtrzSH are noted in the structure of $[Cd(HtrzSH)_2Cl_2]_n$ (LOFJEW; Zhang *et al.*, 2008), *i.e.* monodentate, as for the above, as well as bidentate, μ_2-bridging as one of the triazolyl-N atoms also coordinates Cd^{II} in this polymeric structure. In the final structure with HtrzSH, tridentate coordination for HtrzSH *via* the thione-S atom only has been observed in $[Ag(HtrzSH)Cl]_n$ (XINDUV; Kang *et al.*, 2013), which is a two-dimensional coordination polymer.

As indicated above for $Fe(NO)_2(HtrzS)(HtrzSH)\cdot 0.5H_2O$ (EYABOV01; Aldoshin *et al.*, 2008), mono-anionic forms of HtrzSH are known. Here, HtrzS functions as a monodentate thiolate-S ligand. A monodentate thiolate-S mode of coordination is also seen in $(3\text{-}ClC_6H_4CH_2)_3Sn(HtrzS)$ (SUXSAG; Keng *et al.*, 2010). The three remaining structures feature a tridentate coordination mode leading to coordination polymers. In $[Cu(HtrzS)]_n$ (TEHYIQ; Zhang *et al.*, 2012), this is achieved by bidentate, μ_2-bridging by the thiolate-S atom and the participation of one of the triazolyl-N atoms in coordination. In $[Pb(HtrzS)(NO_3)OH_2]_n$ (MOKKAA; Imran *et al.*, 2015), the thiolate-S and two triazolyl-N atoms are involved in coordination. A similar coordination mode is found for one of the independent anions in $[Cd_2(HtrzS)_2(SO_4)]_n$ (LOFJUM; Zhang *et al.*, 2008). The second anion is tetradentate as the thiolate-S atom is bidentate, μ_2-bridging. From the foregoing, it is evident that HtrzSH/HtrzS ligands adopt a wide range of coordination modes in the relatively few structures in which they have been characterized, suggesting further work in this area is warranted.

7. Synthesis and crystallization

Silver nitrate (0.21 g, 1.24 mmol) and potassium thiocyanate (0.12 g, 1.23 mmol) were dissolved in acetronitrile (25 ml) and a white precipitate formed. This mixture was heated at 323–325 K for 30 min. Then, a clear solution of 1*H*-1,2,4-triazole-3-thiol (0.25 g, 2.47 mmol) in distilled water (5 ml) was added followed by heating for 4.3 h during which time the precipitate slowly dissolved. The clear solution was filtered and kept to evaporate at ambient temperature. After a few days, colourless trapezoidal prisms of (I) formed, which were filtered off and dried *in vacuo*. M.p.: 413–417 K. IR (solid KBr pellet, cm^{-1}): 2108 (*s*) (C≡N), 1479 (*s*) (C=N), 1248 (*w*) (C–N), 1054 (*m*) (C—S) + (C—N).

8. Refinement

Crystal data, data collection and structure refinement details are summarized in Table 4. The H atoms were found in difference Fourier maps and their positions refined resulting in distances of N—H = 0.80 (4)–0.877 (10) Å and C—H = 0.89 (4)–0.91 (4) Å, and with $U_{iso}(H) = 1.2U_{eq}(N, C)$. The maximum and minimum residual electron density peaks of 0.96 and 1.04 e $Å^{-3}$, respectively, were located 0.83 and 0.77 Å from the N3 and Ag atoms, respectively.

Table 4
Experimental details.

Crystal data	
Chemical formula	$[Ag_2(SCN)_2(C_2H_3N_3S)_4]$
M_r	736.44
Crystal system, space group	Monoclinic, $P2_1/n$
Temperature (K)	100
a, b, c (Å)	4.8718 (1), 15.9511 (1), 13.9575 (1)
β (°)	96.945 (1)
V ($Å^3$)	1076.69 (2)
Z	2
Radiation type	Cu $K\alpha$
μ (mm^{-1})	20.35
Crystal size (mm)	0.41 × 0.14 × 0.11
Data collection	
Diffractometer	Rigaku Oxford Diffraction SuperNova, Dual, Cu at zero, AtlasS2
Absorption correction	Gaussian (*CrysAlis PRO*; Rigaku OD, 2015)
T_{min}, T_{max}	0.097, 0.453
No. of measured, independent and observed [$I > 2\sigma(I)$] reflections	18122, 2266, 2242
R_{int}	0.039
$(\sin\theta/\lambda)_{max}$ ($Å^{-1}$)	0.633
Refinement	
$R[F^2 > 2\sigma(F^2)]$, $wR(F^2)$, S	0.025, 0.066, 1.17
No. of reflections	2266
No. of parameters	163
No. of restraints	10
H-atom treatment	Only H-atom coordinates refined
$\Delta\rho_{max}$, $\Delta\rho_{min}$ (e $Å^{-3}$)	0.96, −1.04

Computer programs: *CrysAlis PRO* (Rigaku OD, 2015), *SHELXT* (Sheldrick, 2015), *SHELXL2014/7* (Sheldrick, 2015), *Mercury* (Macrae *et al.*, 2008), *DIAMOND* (Brandenburg, 2006), *WinGX* (Farrugia, 2012) and *publCIF* (Westrip, 2010).

Funding information

We are grateful for financial support from the Research and Development Office, Prince of Songkla University (SCI570390S), the Center for Innovation in Chemistry (PERCH–CIC), the Commission on Higher Education, the Ministry of Education and Department of Chemistry, Faculty of Science, PSU. Sunway University Sdn Bhd is also thanked for financial support of this work through Grant No. STR-RCTR-RCCM-001–2019.

References

Aldoshin, S. M., Lyssenko, K. A., Antipin, M. Yu., Sanina, N. A. & Gritsenko, V. V. (2008). *J. Mol. Struct.* **875**, 309–315.
Almasirad, A., Tabatabai, S. A., Faizi, M., Kebriaeezadeh, A., Mehrabi, N., Dalvandi, A. & Shafiee, A. (2004). *Bioorg. Med. Chem. Lett.* **14**, 6057–6059.
Al-Soud, Y. A., Al-Masoudi, N. A. & Ferwanah, A. E. S. (2003). *Bioorg. Med. Chem.* **11**, 1701–1708.
Altundas, A., Sarı, N., Colak, N. & Ögütcü, H. (2010). *Med. Chem. Res.* **19**, 576–588.
Amer, S., El-Wakiel, N. & El-Ghamry, H. (2013). *J. Mol. Struct.* **1049**, 326–335.
Amir, M. & Shikha, K. (2004). *Eur. J. Med. Chem.* **39**, 535–545.
Bheeter, S. R., Rajalakshmi, R. T., Vasanth, N. & Dons, T. (2016). *Int. J. Appl. Res. (Delhi)*, **2**, 760–763.

Brandenburg, K. (2006). *DIAMOND*. Crystal Impact GbR, Bonn, Germany.
Büyükekşi, S. I., Erkısa, M., Şengül, A., Ulukaya, E. & Oral, A. Y. (2018). *Appl. Organomet. Chem.* **32**, e4406.
Dharmaraj, N., Viswanathamurthi, P. & Natarajan, K. (2001). *Transit. Met. Chem.* **26**, 105–109.
Farrugia, L. J. (2012). *J. Appl. Cryst.* **45**, 849–854.
Groom, C. R., Bruno, I. J., Lightfoot, M. P. & Ward, S. C. (2016). *Acta Cryst.* B**72**, 171–179.
Imran, M., Mix, A., Neumann, B., Stammler, H.-G., Monkowius, U., Gründlinger, P. & Mitzel, N. W. (2015). *Dalton Trans.* **44**, 924–937.
Kang, X.-P., Hu, Y.-S., Zhu, L.-H. & An, Z. (2013). *Inorg. Chem. Commun.* **29**, 169–171.
Keng, T. C., Lo, K. M. & Ng, S. W. (2010). *Acta Cryst.* E**66**, m1064.
Kodcharat, K., Pakawatchai, C. & Saithong, S. (2013). *Acta Cryst.* E**69**, m265–m266.
Liang, Q., Wang, Y.-L., Zhao, Y. & Cao, G.-J. (2014). *Acta Cryst.* C**70**, 182–184.
Macrae, C. F., Bruno, I. J., Chisholm, J. A., Edgington, P. R., McCabe, P., Pidcock, E., Rodriguez-Monge, L., Taylor, R., van de Streek, J. & Wood, P. A. (2008). *J. Appl. Cryst.* **41**, 466–470.
McKinnon, J. J., Spackman, M. A. & Mitchell, A. S. (2004). *Acta Cryst.* B**60**, 627–668.
Parr, R. G. & Yang, W. (1994). *Density-Functional Theory of Atoms and Molecules*. Oxford University Press.
Rigaku OD (2015). *CrysAlis PRO*. Rigaku Oxford Diffraction, Yarnton, England.
Sheldrick, G. M. (2015). *Acta Cryst.* C**71**, 3–8.
Singh, K., Singh, D. P., Barwa, M. S., Tyagi, P. & Mirza, Y. (2006). *J. Enzyme Inhib. Med. Chem.* **21**, 557–562.
Tan, S. L., Jotani, M. M. & Tiekink, E. R. T. (2019). *Acta Cryst.* E**75**, 308–318.
Turan-Zitouni, G., Kaplancıklı, Z. A., Yıldız, M. T., Chevallet, P. & Kaya, D. (2005). *Eur. J. Med. Chem.* **40**, 607–613.
Turner, M. J., McKinnon, J. J., Wolff, S. K., Grimwood, D. J., Spackman, P. R., Jayatilaka, D. & Spackman, M. A. (2017). *Crystal Explorer 17*. University of Western Australia.
Valiev, M., Bylaska, E. J., Govind, N., Kowalski, K., Straatsma, T. P., Van Dam, H. J. J., Wang, D., Nieplocha, J., Apra, E., Windus, T. L. & de Jong, W. A. (2010). *Comput. Phys. Commun.* **181**, 1477–1489.
Walczak, K., Gondela, A. & Suwiński, J. (2004). *Eur. J. Med. Chem.* **39**, 849–853.
Wani, K., Pakawatchai, C. & Saithong, S. (2013). *Acta Cryst.* E**69**, m34–m35.
Wattanakanjana, Y., Palamae, S., Ratthiwan, J. & Nimthong, R. (2014). *Acta Cryst.* E**70**, m61–m62.
Westrip, S. P. (2010). *J. Appl. Cryst.* **43**, 920–925.
Zhang, R.-B., Li, Z.-J., Cheng, J.-K., Qin, Y.-Y., Zhang, J. & Yao, Y.-G. (2008). *Cryst. Growth Des.* **8**, 2562–2573.
Zhang, X., Cheng, J.-K., Zhang, M.-J. & Yao, Y.-G. (2012). *Inorg. Chem. Commun.* **20**, 101–104.

supporting information

Acta Cryst. (2020). E**76**, 42-47 [https://doi.org/10.1107/S2056989019016359]

Crystal and molecular structures of a binuclear mixed ligand complex of silver(I) with thiocyanate and 1*H*-1,2,4-triazole-5(4*H*)-thione

Janjira Kreaunakpan, Kittipong Chainok, Nathan R. Halcovitch, Edward R. T. Tiekink, Teerapong Pirojsirikul and Saowanit Saithong

Computing details

Data collection: *CrysAlis PRO* (Rigaku OD, 2015); cell refinement: *CrysAlis PRO* (Rigaku OD, 2015); data reduction: *CrysAlis PRO* (Rigaku OD, 2015); program(s) used to solve structure: ShelXT (Sheldrick, 2015); program(s) used to refine structure: *SHELXL2014/7* (Sheldrick, 2015); molecular graphics: *Mercury* (Macrae *et al.*, 2008), *DIAMOND* (Brandenburg, 2006); software used to prepare material for publication: *WinGX* (Farrugia, 2012) and *publCIF* (Westrip, 2010).

Bis[μ-1*H*-1,2,4-triazole-5(4*H*)-thione-κ^2*S*:*S*]bis{(thiocyanato-κ*S*)[1*H*-1,2,4-triazole-5(4*H*)-thione-κ*S*]silver(I)}

Crystal data

$[Ag_2(SCN)_2(C_2H_3N_3S)_4]$
M_r = 736.44
Monoclinic, $P2_1/n$
a = 4.8718 (1) Å
b = 15.9511 (1) Å
c = 13.9575 (1) Å
β = 96.945 (1)°
V = 1076.69 (2) Å^3
Z = 2
$F(000)$ = 720
D_x = 2.272 Mg m^{-3}
Cu $K\alpha$ radiation, λ = 1.54184 Å
Cell parameters from 13766 reflections
θ = 3.2–77.1°
μ = 20.35 mm^{-1}
T = 100 K
Prism, colourless
0.41 × 0.14 × 0.11 mm

Data collection

Rigaku Oxford Diffraction SuperNova, Dual, Cu at zero, AtlasS2 diffractometer
Mirror monochromator
Detector resolution: 5.2303 pixels mm^{-1}
ω scans
Absorption correction: gaussian (CrysAlisPro; Rigaku OD, 2015)
T_{min} = 0.097, T_{max} = 0.453
18122 measured reflections
2266 independent reflections
2242 reflections with $I > 2\sigma(I)$
R_{int} = 0.039
θ_{max} = 77.4°, θ_{min} = 4.2°
h = −6→5
k = −19→20
l = −17→17

Refinement

Refinement on F^2
Least-squares matrix: full
$R[F^2 > 2\sigma(F^2)]$ = 0.025
$wR(F^2)$ = 0.066
S = 1.17
2266 reflections
163 parameters
10 restraints
Primary atom site location: structure-invariant direct methods
Secondary atom site location: difference Fourier map

Hydrogen site location: difference Fourier map
Only H-atom coordinates refined
$w = 1/[\sigma^2(F_o^2) + (0.0343P)^2 + 1.905P]$
where $P = (F_o^2 + 2F_c^2)/3$

$(\Delta/\sigma)_{max} = 0.001$
$\Delta\rho_{max} = 0.96$ e Å^{-3}
$\Delta\rho_{min} = -1.04$ e Å^{-3}

Special details

Geometry. All esds (except the esd in the dihedral angle between two l.s. planes) are estimated using the full covariance matrix. The cell esds are taken into account individually in the estimation of esds in distances, angles and torsion angles; correlations between esds in cell parameters are only used when they are defined by crystal symmetry. An approximate (isotropic) treatment of cell esds is used for estimating esds involving l.s. planes.

Refinement. C5 treated with ISOR

Fractional atomic coordinates and isotropic or equivalent isotropic displacement parameters (Å²)

	x	*y*	*z*	U_{iso}*/U_{eq}
Ag	0.56775 (4)	0.42032 (2)	0.59899 (2)	0.01119 (9)
S1	0.81885 (13)	0.55635 (4)	0.56609 (4)	0.00788 (14)
S2	0.81257 (13)	0.29260 (4)	0.54731 (4)	0.00780 (14)
S3	0.25779 (15)	0.43047 (4)	0.73213 (5)	0.01162 (15)
N1	0.4853 (5)	0.63635 (14)	0.68422 (16)	0.0077 (4)
H1N	0.390 (6)	0.5923 (15)	0.698 (3)	0.009*
N2	0.4273 (5)	0.71516 (14)	0.71587 (16)	0.0097 (4)
N3	0.7598 (5)	0.71790 (14)	0.62260 (16)	0.0082 (4)
H3N	0.885 (5)	0.735 (2)	0.587 (2)	0.010*
N4	0.4504 (5)	0.19814 (14)	0.63991 (16)	0.0087 (4)
H4N	0.369 (8)	0.236 (2)	0.663 (3)	0.010*
N5	0.3865 (5)	0.11639 (15)	0.65884 (17)	0.0117 (5)
N6	0.7280 (5)	0.12487 (14)	0.56881 (16)	0.0089 (4)
H6N	0.854 (5)	0.111 (2)	0.532 (2)	0.011*
N7	0.5604 (6)	0.40606 (16)	0.91561 (18)	0.0150 (5)
C1	0.6846 (5)	0.63623 (16)	0.62603 (18)	0.0070 (5)
C2	0.5982 (6)	0.76322 (17)	0.67677 (19)	0.0093 (5)
H2	0.615 (7)	0.818 (2)	0.688 (2)	0.011*
C3	0.6577 (6)	0.20539 (16)	0.58544 (18)	0.0076 (5)
C4	0.5594 (6)	0.07362 (17)	0.6139 (2)	0.0110 (6)
H4	0.571 (7)	0.017 (3)	0.612 (2)	0.013*
C5	0.4422 (6)	0.41636 (15)	0.8389 (2)	0.0089 (5)

Atomic displacement parameters (Å²)

	U^{11}	U^{22}	U^{33}	U^{12}	U^{13}	U^{23}
Ag	0.01970 (15)	0.00638 (12)	0.00859 (12)	0.00126 (7)	0.00616 (8)	−0.00024 (6)
S1	0.0112 (3)	0.0055 (3)	0.0077 (3)	0.0013 (2)	0.0041 (2)	−0.0004 (2)
S2	0.0108 (3)	0.0057 (3)	0.0078 (3)	0.0001 (2)	0.0048 (2)	0.0008 (2)
S3	0.0137 (4)	0.0139 (3)	0.0078 (3)	−0.0011 (2)	0.0037 (2)	0.0010 (2)
N1	0.0106 (11)	0.0055 (10)	0.0080 (10)	−0.0009 (8)	0.0056 (8)	−0.0010 (8)
N2	0.0125 (12)	0.0072 (10)	0.0101 (11)	−0.0003 (9)	0.0043 (9)	−0.0023 (8)
N3	0.0112 (12)	0.0057 (10)	0.0085 (10)	−0.0012 (8)	0.0046 (8)	−0.0004 (8)
N4	0.0116 (12)	0.0047 (10)	0.0112 (11)	0.0016 (9)	0.0063 (9)	0.0005 (8)

N5	0.0142 (12)	0.0078 (11)	0.0139 (11)	−0.0003 (9)	0.0053 (9)	0.0018 (8)
N6	0.0113 (12)	0.0070 (10)	0.0094 (10)	0.0019 (9)	0.0051 (8)	0.0002 (8)
N7	0.0191 (14)	0.0151 (11)	0.0118 (12)	−0.0019 (10)	0.0064 (10)	0.0013 (9)
C1	0.0087 (13)	0.0075 (12)	0.0045 (11)	0.0001 (9)	0.0001 (9)	0.0014 (9)
C2	0.0118 (14)	0.0069 (12)	0.0097 (12)	−0.0002 (10)	0.0029 (10)	−0.0026 (9)
C3	0.0096 (13)	0.0090 (12)	0.0042 (11)	0.0016 (10)	0.0007 (9)	0.0000 (9)
C4	0.0154 (16)	0.0070 (13)	0.0111 (13)	−0.0016 (10)	0.0034 (11)	0.0017 (9)
C5	0.0093 (9)	0.0086 (8)	0.0096 (9)	−0.0006 (7)	0.0041 (7)	−0.0005 (7)

Geometric parameters (Å, º)

Ag—S1	2.5596 (7)	N3—C2	1.363 (3)
Ag—S2	2.5103 (6)	N3—H3N	0.877 (10)
Ag—S3	2.5374 (7)	N4—C3	1.341 (3)
Ag—S1^{i}	2.8188 (7)	N4—N5	1.374 (3)
C1—S1	1.698 (3)	N4—H4N	0.80 (4)
S1—Ag^{i}	2.8188 (7)	N5—C4	1.302 (4)
C3—S2	1.698 (3)	N6—C3	1.357 (3)
C5—S3	1.660 (3)	N6—C4	1.365 (4)
N1—C1	1.339 (3)	N6—H6N	0.878 (7)
N1—N2	1.373 (3)	N7—C5	1.164 (4)
N1—H1N	0.878 (10)	C2—H2	0.89 (4)
N2—C2	1.299 (4)	C4—H4	0.91 (4)
N3—C1	1.356 (3)		

S1—Ag—S2	112.49 (2)	C3—N4—H4N	127 (3)
S1—Ag—S3	114.64 (2)	N5—N4—H4N	120 (3)
S1—Ag—S1^{i}	91.60 (2)	C4—N5—N4	103.3 (2)
S2—Ag—S3	127.43 (2)	C3—N6—C4	108.0 (2)
S2—Ag—S1^{i}	99.56 (2)	C3—N6—H6N	123 (2)
S3—Ag—S1^{i}	101.08 (2)	C4—N6—H6N	128 (2)
C1—S1—Ag	109.08 (9)	N1—C1—N3	103.8 (2)
C1—S1—Ag^{i}	92.55 (9)	N1—C1—S1	130.6 (2)
Ag—S1—Ag^{i}	88.40 (2)	N3—C1—S1	125.6 (2)
C3—S2—Ag	109.28 (9)	N2—C2—N3	111.3 (2)
C5—S3—Ag	110.08 (10)	N2—C2—H2	124 (2)
C1—N1—N2	112.9 (2)	N3—C2—H2	124 (2)
C1—N1—H1N	125 (2)	N4—C3—N6	103.8 (2)
N2—N1—H1N	122 (2)	N4—C3—S2	129.9 (2)
C2—N2—N1	103.8 (2)	N6—C3—S2	126.2 (2)
C1—N3—C2	108.3 (2)	N5—C4—N6	111.6 (2)
C1—N3—H3N	122 (2)	N5—C4—H4	126 (2)
C2—N3—H3N	130 (2)	N6—C4—H4	122 (2)
C3—N4—N5	113.3 (2)	N7—C5—S3	176.9 (3)

C1—N1—N2—C2	−0.8 (3)	N1—N2—C2—N3	−0.2 (3)
C3—N4—N5—C4	−0.4 (3)	C1—N3—C2—N2	1.0 (3)
N2—N1—C1—N3	1.4 (3)	N5—N4—C3—N6	0.2 (3)

N2—N1—C1—S1	−177.4 (2)	N5—N4—C3—S2	−177.8 (2)
C2—N3—C1—N1	−1.4 (3)	C4—N6—C3—N4	0.1 (3)
C2—N3—C1—S1	177.5 (2)	C4—N6—C3—S2	178.2 (2)
Ag—S1—C1—N1	1.2 (3)	Ag—S2—C3—N4	−4.3 (3)
Ag^{i}—S1—C1—N1	90.4 (3)	Ag—S2—C3—N6	178.2 (2)
Ag—S1—C1—N3	−177.4 (2)	N4—N5—C4—N6	0.4 (3)
Ag^{i}—S1—C1—N3	−88.2 (2)	C3—N6—C4—N5	−0.4 (3)

Symmetry code: (i) −*x*+1, −*y*+1, −*z*+1.

Hydrogen-bond geometry (Å, º)

D—H···*A*	*D*—H	H···*A*	*D*···*A*	*D*—H···*A*
N1—H1*N*···S3	0.88 (1)	2.72 (2)	3.555 (2)	161 (3)
N1—H1*N*···N5^{ii}	0.88 (3)	2.57 (4)	3.023 (3)	113
N3—H3*N*···S2^{iii}	0.88 (1)	2.56 (2)	3.345 (2)	150 (3)
N4—H4*N*···N2^{iv}	0.80 (4)	2.38 (4)	2.900 (3)	123 (3)
N6—H6*N*···N7^{v}	0.88 (1)	2.03 (1)	2.877 (3)	163 (3)
C2—H2···S3^{ii}	0.89 (4)	2.87 (4)	3.504 (3)	129 (3)
C2—H2···N7^{vi}	0.89 (4)	2.66 (3)	3.184 (4)	118 (3)
C4—H4···N7^{vii}	0.91 (4)	2.58 (4)	3.306 (4)	137 (3)

Symmetry codes: (ii) −*x*+1/2, *y*+1/2, −*z*+3/2; (iii) −*x*+2, −*y*+1, −*z*+1; (iv) −*x*+1/2, *y*−1/2, −*z*+3/2; (v) *x*+1/2, −*y*+1/2, *z*−1/2; (vi) −*x*+3/2, *y*+1/2, −*z*+3/2; (vii) −*x*+3/2, *y*−1/2, −*z*+3/2.